PHYSICAL REVIEW B **105**, 115127 (2022)

Harmonically confined N-electron systems coupled to light in a cavity

Justin Malave, Yetmgeta S. Aklilu, Matthew Beutel, Chenhang Huang, and Kálmán Varga [*]
Department of Physics and Astronomy, Vanderbilt University, Nashville, Tennessee, 37235, USA

(Received 11 February 2022; revised 1 March 2022; accepted 9 March 2022; published 21 March 2022)

The energy and wave function of a harmonically confined N-electron system coupled to light is calculated by separating the wave functions of the relative and center-of-mass (CM) motions. The light only couples to the CM variable, and the coupled equation can be solved analytically. The relative motion wave function has to be numerically approximated, but the relative Hamiltonian is independent of the coupling strength and it only gives a shift in the energy. The approach works for any coupling strength and the effective coupling strength can be increased by increasing the number of electrons. This gives an extra degree of freedom to fine tune the resonances and other properties of the light-matter coupled systems. Examples of wave functions of light-matter hybrid states are presented.

DOI: 10.1103/PhysRevB.105.115127

I. INTRODUCTION

Light-matter interactions in optical cavities have been intensely studied in the last two decades. Strong coupling between cavity electromagnetic modes and atoms or molecules can lead to a formation of hybrid light-matter states (polaritons), combining the properties of their ingredients. The properties of these hybrid systems are significantly different from that of the original molecule or atom. The coupling leads to the modification of potential energy surfaces, charge states, reactivity, and structure. This possibility has attracted enormous experimental [1–11]. (See, e.g., Ref. [12] for more references) and theoretical interest [13–49].

Model systems with simple analytical solutions have always played important roles in understanding complex physical systems and in testing numerical methods. The interaction of light and atoms, for example, can be described by the Jaynes-Cummings model [50], which assumes a two-level atom is weakly coupled to a single mode of a quantized electromagnetic field. For strongly coupled light-matter systems [19–23,25,29,36,39,46,47,51–54] no simple approach exists and the light-matter coupling cannot be treated perturbatively either.

We will consider a harmonically confined system of electrons. Quantum confinement is often modeled by a parabolic quantum well [55], or by a harmonic trap [56–58]. Electrons in magnetic fields are also subject to a harmonic confinement [67]. The quadratic potential allows the separation of the center-of-mass (CM) and relative motion and the electric field only couples to the CM wave function (harmonic potential theorem) [59–64].

In a previous paper [65], we developed an analytical solution for a harmonically confined two-electron system interacting with light in a cavity. In this system, the wave function can be written as a product of the wave functions of the relative and CM motion. The relative motion wave function can be expanded into an infinite series. For certain oscillator parameters, this infinite series can be reduced to a recursion [66] giving an analytical solution. The wave function of the center-of-mass motion can also be calculated analytically.

In this paper, we generalize the two-electron solution to N electrons. The relative and the CM wave function can be separated in the same way as in the two-electron case, but the relative Hamiltonian can no longer be analytically solved. This work, in some sense, is the generalization of the harmonic potential theorem to quantized electromagnetic fields. The photons are only coupled to the CM coordinate, and the coupled CM photon system can be solved exactly using shifted Fock states. The relative Hamiltonian can be solved approximately using numerical approaches, two of which will be presented and compared here.

The first one, stochastic variational method (SVM) [67,68] can be used to solve few-electron problems [69–72] and it has been recently generalized for light-matter coupled states [73]. The SVM generates optimized light-matter coupled wave function using a product of explicitly correlated Gaussian (ECG) basis [74] states and photon Fock states. The stochastic parameter selection keeps the basis dimension and the computational cost manageable by avoiding the high-dimensional tensor product spaces. The advantage of the approach is that the matrix elements are analytically available [67,75–77] and it allows very accurate calculations of energies and physical properties [69,78–80]. The SVM approach scales with $N!$ for an N-electron system and it can only be used to small number of particles.

The second approach for the relative motion uses a density functional theory (DFT) [81,82] Hamiltonian for the relative part. Unlike SVM, the DFT is not limited to small systems, but its accuracy is not as good as the correlated basis approach used in SVM. DFT calculations have often been used to analyze the structure and energetics of confined electron systems and Wigner crystals [81–89].

---

[*] kalman.varga@vanderbilt.edu

©2022 American Physical Society

II. FORMALISM

We assume that the system is nonrelativistic and the coupling to the light can be described by the dipole approximation (the wavelength of light is much larger than the size of the system). The Pauli-Fierz (PF) nonrelativistic quantum electrodynamics (QED) Hamiltonian provides a consistent quantum description at this level. The PF Hamiltonian in the Coulomb gauge [21,25,38,46,51]: $H = H_e + H_{ep}$ where H_e is the electronic Hamiltonian and

$$H_{ep} = \sum_{\alpha=1}^{N_p} \left[\omega_\alpha \left(\hat{a}_\alpha^+ \hat{a}_\alpha + \frac{1}{2} \right) - \omega_\alpha q_\alpha \boldsymbol{\lambda}_\alpha \mathbf{D} + \frac{1}{2} (\boldsymbol{\lambda}_\alpha \mathbf{D})^2 \right] \quad (1)$$

describes the interaction of electrons and photons (atomic units are used in this work). In Eq. (1) the photon fields are described by quantized oscillators using raising and lowering operators $\hat{a}_\alpha$ and $\hat{a}_\alpha^+$, $\mathbf{D}$ is the dipole operator, and

$$q_\alpha = \frac{1}{\sqrt{2\omega_\alpha}} (\hat{a}_\alpha^+ + \hat{a}_\alpha) \quad (2)$$

is the displacement field. This Hamiltonian describes N_p photon modes with photon frequency ω_α and coupling $\boldsymbol{\lambda}_\alpha$. The coupling term is usually written as [90] $\boldsymbol{\lambda}_\alpha = \sqrt{4\pi}\, S_\alpha(\mathbf{r})\mathbf{e}_\alpha$, where $S_\alpha(\mathbf{r})$ is the cavity mode function at position $\mathbf{r}$ and $\mathbf{e}_\alpha$ is the transversal polarization vector of the photon modes. The first term in Eq. (1) is the Hamiltonian of the photon modes, the second term couples the photons to the dipole and the last term is the dipole self-interaction, $H_d = \frac{1}{2}\sum_{\alpha=1}^{N_p} (\boldsymbol{\lambda}_\alpha \mathbf{D})^2$.

A. Electronic Hamiltonian

We consider an N-electron system confined in a harmonic oscillator potential interacting with a Coulomb potential

$$H_e = \frac{1}{2}\sum_{i=1}^{N} \mathbf{p}_i^2 + \frac{1}{2}\omega_0^2 \sum_{i=1}^{N} \mathbf{r}_i^2 + \frac{1}{2}\sum_{i<j}^{N} \frac{1}{|\mathbf{r}_i - \mathbf{r}_j|}, \quad (3)$$

where $\mathbf{r}_i$ are the position of electrons. By defining the relative coordinates

$$\mathbf{x}_i = \mathbf{r}_i - \mathbf{R}, \quad \mathbf{R} = \frac{1}{N}\sum_{i=1}^{N} \mathbf{r}_i, \quad (4)$$

the Hamiltonian can be written as

$$H_e = H_{\mathbf{x}} + H_{\mathbf{R}}, \quad (5)$$

with

$$H_{\mathbf{x}} = \frac{1}{2}\sum_{i=1}^{N-1} \boldsymbol{\pi}_i^2 + \frac{1}{2}\frac{\omega_0^2}{N}\sum_{i<j}^{N} (\mathbf{x}_i - \mathbf{x}_j)^2 + \frac{1}{2}\sum_{i<j}^{N} \frac{1}{|\mathbf{x}_i - \mathbf{x}_j|}, \quad (6)$$

and

$$H_{\mathbf{R}} = \frac{1}{2N}\mathbf{P}^2 + \frac{1}{2}N\omega_0^2 \mathbf{R}^2, \quad (7)$$

where $\mathbf{P}$ is the canonically conjugate momentum to $\mathbf{R}$ and $\boldsymbol{\pi}_i$ are canonically conjugate momenta to $\mathbf{x}_i$ (only $N-1$ of these are linearly independent).

B. Electron-photon coupling Hamiltonian

Assuming that we have only one photon mode and define the coupling term as $\boldsymbol{\lambda} = \lambda(1, 1, 0)$ and the dipole operator as

$$\mathbf{D} = \sum_{i=1}^{N} \mathbf{r}_i, \quad (8)$$

the electron-photon coupling term becomes

$$H_{ep} = \omega\left(\hat{a}^+\hat{a} + \frac{1}{2}\right) - N\omega q \boldsymbol{\lambda}\mathbf{R} + \frac{1}{2}N^2(\boldsymbol{\lambda}\mathbf{R})^2. \quad (9)$$

C. Decoupling the relative and center-of-mass Hamiltonian

Now the total Hamiltonian can be written as

$$H = H_{\mathbf{x}} + \omega\left(\hat{a}^+\hat{a} + \frac{1}{2}\right) - N\omega q \boldsymbol{\lambda}\mathbf{R} + \left(H_{\mathbf{R}} + \frac{1}{2}N^2(\boldsymbol{\lambda}\mathbf{R})^2\right). \quad (10)$$

The first term is the Hamiltonian of the relative motion and it is not coupled to the center-of-mass motion or to the photon space. The second term is the Hamiltonian of the photon, which is coupled to the center of mass through the third term. The last term in the parenthesis is the Hamiltonian acting on the center-of-mass motion.

D. Decoupling the center-of-mass Hamiltonian

The center-of-mass part can be simplified further by introducing

$$u = \sqrt{N}\frac{X+Y}{\sqrt{2}}, \quad v = \sqrt{N}\frac{Y-X}{\sqrt{2}}, \quad z = \sqrt{N}Z, \quad (11)$$

where $\mathbf{R} = (X, Y, Z)$. Now we have

$$H_{\mathbf{R}} + \frac{1}{2}N^2(\boldsymbol{\lambda}\mathbf{R})^2 = H_u + H_v + H_z, \quad (12)$$

with

$$H_u = -\frac{1}{2}\frac{\partial^2}{\partial u^2} + \frac{1}{2}\omega_u^2 u^2, \quad (13)$$

and H_v and H_z are similarly defined harmonic oscillator Hamiltonians with

$$\omega_u^2 = \omega_0^2 + 2N\lambda^2, \quad \omega_v^2 = \omega_z^2 = \omega_0^2. \quad (14)$$

This gives three independent harmonic oscillators, and only H_u is coupled to the light. This derivation can be easily generalized to any form of $\boldsymbol{\lambda}$ [65], and not limited to the present $\boldsymbol{\lambda} = \lambda(1, 1, 0)$ choice.

The solution for H_v and H_z is trivial,

$$H_v\phi_k(v) = \left(k + \frac{1}{2}\right)\omega_u\phi_k(v), \quad (15)$$

and

$$H_z\phi_l(z) = \left(l + \frac{1}{2}\right)\omega_z\phi_l(z), \quad (16)$$

where $\phi_k(v)$ and $\phi_l(z)$ are harmonic oscillator eigenfunctions.

E. Light-CM coupling

Now we can define a simplified coupling Hamiltonian in the following form:

$$H_c = \omega\left(\hat{a}^{+}\hat{a} + \frac{1}{2}\right) - \omega q\lambda' u + H_u, \tag{17}$$

where $\lambda' = \sqrt{2N}\lambda$. The total Hamiltonian now becomes

$$H = H_{\mathbf{x}} + H_v + H_z + H_c, \tag{18}$$

with eigenenergies

$$E = E_{\mathbf{x}} + E_v + E_z + E_c. \tag{19}$$

The Hamiltonian is sum of four uncoupled terms and can be diagonalized by using a product ansatz

$$\Phi(\mathbf{x})\phi_k(v)\phi_l(z)\Phi_c(u), \tag{20}$$

where $\Phi(\mathbf{x})$, $\phi_k(v)$, $\phi_l(z)$ and $\Phi_c(u)$ are the eigenfunctions of the four Hamiltonians. The last three are analytically solvable while some approximation or numerical solution is needed for the first Hamiltonian.

III. DIAGONALIZATION OF THE LIGHT-MATTER COUPLED HAMILTONIAN

This section is a generalization of the two-particle case [65] to N electrons. The extension to more than one photon mode is straightforward and presented in the Appendix.

The Hamiltonian H_c can be diagonalized in two different ways. In the first approach, new variables are introduced to decouple the CM and photon harmonic oscillators. In the second one, a product basis of the CM and photon harmonic oscillators, $\phi_k(u)|n>$ is used, where $\phi_k(u)$ satisfies

$$H_u\phi_k(u) = \left(k + \frac{1}{2}\right)\omega_u\phi_k(u). \tag{21}$$

The advantage of the first approach is that it is exact, while numerical diagonalization is needed in the second approach. The advantage of the second approach is that the solution is directly obtained as a product of spatial and photon spaces.

A. Shifted Fock states

We first introduce the following coordinate rotations:

$$s = usin(\alpha) + q\cos(\alpha), \tag{22}$$

$$t = -u\cos(\alpha) + q\sin(\alpha), \tag{23}$$

and choose α so that the coupling term of the Hamiltonian H_c is eliminated and the Hamiltonian simplifies to a sum of the uncoupled harmonic oscillators

$$H_c = \left(-\frac{1}{2}\frac{\partial^2}{\partial s^2} + \frac{1}{2}\omega_s^2 s^2\right) + \left(-\frac{1}{2}\frac{\partial^2}{\partial t^2} + \frac{1}{2}\omega_t^2 t^2\right). \tag{24}$$

1. Harmonic confinement

For arbitrary ω_0, ω, and λ' one can decouple s and t by setting

$$\tan(2\alpha) = \frac{2\omega\lambda'}{\chi}, \quad \chi = \omega_u^2 - \omega^2, \tag{25}$$

and the harmonic oscillator frequencies are

$$\omega_s = |\sin(\alpha)|\sqrt{\omega_0^2 + \left(\lambda' - \frac{\omega}{\tan(\alpha)}\right)^2}, \tag{26}$$

and

$$\omega_t = |\cos(\alpha)|\sqrt{\omega_0^2 + [\lambda' + \omega\tan(\alpha)]^2}. \tag{27}$$

The value of ω_s and ω_t depends on ω_0, ω and λ'. At $\omega = \omega_u$ ($\chi = 0$), $\tan(2\alpha)$ becomes undefined and ω_s and ω_t are switched. When $\chi \to 0_+$ then $\alpha \to \pi/4$ and

$$\omega_s = \omega\sqrt{1 - \lambda'/\omega}, \tag{28}$$

$$\omega_t = \omega\sqrt{1 + \lambda'/\omega} \tag{29}$$

and the transition frequency between the two levels is

$$\omega_t - \omega_s = \lambda' = \sqrt{2N}\lambda. \tag{30}$$

If $\chi \to 0_-$ then $\alpha \to -\pi/4$ and ω_t and ω_s are switched.

2. $\omega_0 \approx 0$ *case*

This is a special case, which will always be reached when the number of particles are increased for a given ω_0. We will refer this as $\omega_0 \approx 0$ case, and we will call the previous case as harmonic confinement. The harmonic potential can never be exactly zero because at least a weak confinement is needed to keep the relative motion bound. The $\omega_0 \approx 0$ is introduced to emphasizes that harmonic confinement does not play a role in the CM coupling.

In this case $\omega_u \approx \lambda'$ and one can derive simpler expressions for ω_s and ω_t using Eqs. (22) and (23). If $\omega < \lambda'$ then

$$\omega_s = 0, \quad \omega_t = (\lambda'^2 + \omega^2)^{1/2}, \tag{31}$$

$$s = \frac{\lambda' q + \omega u}{(\lambda'^2 + \omega^2)^{1/2}}, \quad t = \frac{\omega q - \lambda' u}{(\lambda'^2 + \omega^2)^{1/2}}. \tag{32}$$

If $\lambda' < \omega$ then

$$\omega_s = (\lambda'^2 + \omega^2)^{1/2}, \quad \omega_t = 0, \tag{33}$$

$$s = \frac{\omega q + \lambda' u}{(\lambda'^2 + \omega^2)^{1/2}}, \quad t = \frac{\lambda' q - \omega u}{(\lambda'^2 + \omega^2)^{1/2}}. \tag{34}$$

The light q and the center-of-mass u coordinates are coupled in coordinates s and t. For $\lambda = 0$, $s = \sqrt{\omega}u$ and $t = \sqrt{\omega}q$ and the light and matter are decoupled as expected.

If $\omega < \lambda'$, then as $\omega_s = 0$, the s coordinate does not play a role, and the t coordinate is dominated by u. This will always happen if for a given ω and λ one increases the number of electrons, for large N the electronic u coordinate becomes dominant due to the dipole self-interaction term and the coupling to q. In this case the excitations to higher photon numbers are suppressed.

On the other hand, if $\lambda' < \omega$, then $\omega_t = 0$ and the t coordinate does not play a role, the eigenfunction is a harmonic oscillator function depending on s only. In this case, the q coordinate, the photon excitation will dominate. Examples for this will be presented in the next section where we explicitly diagonalize H_c and the photon q and CM u occupation probabilities will be calculated.

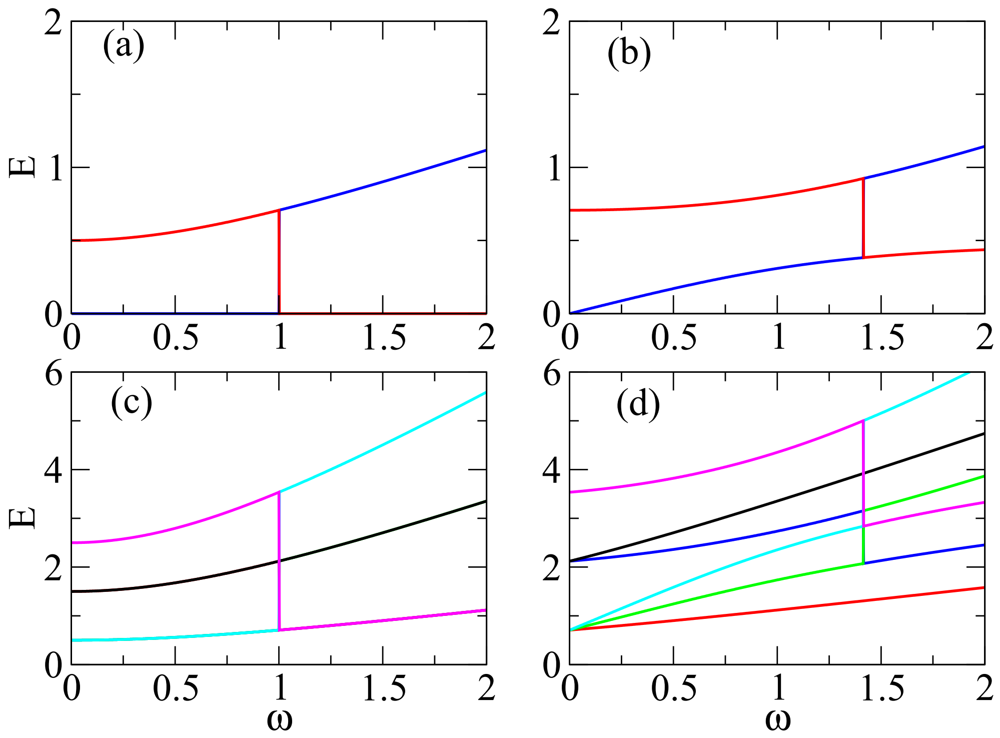

FIG. 1. Eigenenergies of H_c as a function of ω for harmonically confined electrons ($N = 50$) in the shifted Fock space case for $\lambda = 0.1$. (a) ω_s (bottom curve at $\omega = 0$) and ω_t (top curve at $\omega = 0$) in the $\omega_0 \approx 0$ case. (b) ω_s (bottom curve at $\omega = 0$) and ω_t (top curve at $\omega = 0$) for $\omega_0 = 1$. (c) E_c for the $\omega_0 \approx 0$ case with $n_s + n_t \leqslant 5$. If $\omega < \lambda'$ then $\omega_s = 0$, and the lowest curve is $n_t = 0$, the middle curve $n_t = 1$, and the top curve is $n_t = 2$ for any n_s for $\omega < \lambda'$. If $\omega > \lambda'$ then the lowest curve is $n_s = 0$, the middle curve $n_s = 1$, and the upper curve is $n_s = 2$ for any n_t. (d) $E_c =$ for the $\omega_0 = 1$ case with $n_s + n_t \leqslant 5$. In this case there is no degeneracy and one has six lines corresponding to $(n_s, n_t) = (0, 1), (1, 0), (0, 1), (1, 1), (2, 0), (0, 2)$.

3. Numerical examples

Figure 1 shows the eigenenergies of H_c as a function of ω for $N = 50$ and $\lambda = 0.1$. The eigenfrequencies ω_s and ω_t as a function of ω are compared in Fig. 1(a) for the $\omega_0 \approx 0$ case. The frequency ω_s is zero when $\omega < \lambda' = \sqrt{2 \cdot 50 \cdot 0.1^2} = 1$ and at that point ω_s and ω_t are switched and ω_t becomes zero. In the harmonic confinement case [Fig. 1(b)] using $\omega_0 = 1$, ω_s is smaller than ω_t when $\omega < \lambda' = \sqrt{1 + 2 \cdot 50 \cdot 0.1^2} = \sqrt{2}$ but it is not zero. At $\lambda' = \sqrt{2}$ the two frequencies are switched as before.

Figure 1(c) shows the lowest eigenstates

$$E_c = \left(n_s + \frac{1}{2}\right)\omega_s + \left(n_t + \frac{1}{2}\right)\omega_t \tag{35}$$

of H_c, where (n_s, n_t) are integers, for the $\omega_0 \approx 0$ case. For $\omega < \lambda'$ the energy only depends on n_t, otherwise the energy only depends on n_s. This leads to many degenerate states. For example, any $(n_s, n_t = 0)$ pair constitutes a ground state if $\omega < \lambda'$ and any $(n_s = 0, n_t)$ pair is a ground state if $\lambda' < \omega$.

In the harmonic confinement case [Fig. 1(d)], this degeneracy is removed, and the energies of the different (n_s, n_t) pairs are switched to (n_t, n_s) at $\omega = \lambda'$, but $(n_s = 0, n_t = 0)$ is the ground state for all ω.

B. Exact diagonalization

The Hamiltonian in Eq. (17) can also be solved by exact diagonalization using the product of center-of-mass eigenfunctions and photon Fock states as basis states

$$|n_u, n_q\rangle = \phi_{n_u}(u)|n_q\rangle. \tag{36}$$

To diagonalize H_c, one needs the matrix elements of the Hamiltonian, which are readily available. The operators H_u and u act on the real space, and $\hat{a} + \hat{a}^+$ acts on the photon space. The matrix elements of q and u are

$$\langle m|q|n\rangle = \frac{1}{\sqrt{2\omega}} D_{mn}, \tag{37}$$

$$\langle i|u|j\rangle = \frac{1}{\sqrt{2\omega_u}} D_{ij}, \tag{38}$$

where

$$D_{mn} = \begin{pmatrix} 0 & \sqrt{1} & 0 & 0 & 0 & \dots \\ \sqrt{1} & 0 & \sqrt{2} & 0 & 0 & \dots \\ 0 & \sqrt{2} & 0 & \sqrt{3} & 0 & \dots \\ 0 & 0 & \sqrt{3} & 0 & \sqrt{4} & \dots \\ 0 & 0 & 0 & \sqrt{4} & 0 & \dots \\ \vdots & \vdots & \vdots & \vdots & \vdots & \ddots \end{pmatrix}. \tag{39}$$

Thus, the matrix elements of H_c are

$$\langle i,m|H_c|j,n\rangle = \delta_{mn}\delta_{ij}\left(j+\frac{1}{2}\right)\frac{\omega_u}{2} + \delta_{mn}\delta_{ij}\left(n+\frac{1}{2}\right)\omega + \sqrt{\frac{N\omega}{2\omega_u}}\,\lambda\, D_{mn}D_{ij}. \tag{40}$$

After the diagonalization, we have the eigenenergies and the eigenfunctions. The eigenfunction has the following form:

$$\Phi_c = \sum_{n_u,n_q} c_{n_u,n_q}\phi_{n_u}(u)|n_q\rangle, \tag{41}$$

where c_{n_u,n_q} are the components of the eigenvector.

In the large N limit we have $\omega_u \approx \sqrt{2N}\lambda$ and the coupling strength in the last term of Eq. (40) will be

$$\sqrt{\omega}(N/8)^{1/4}, \tag{42}$$

which is independent of λ. In this case, ω_u is very large and the lowest u harmonic oscillator state dominates

$$\Phi_c = \sum_{n_q} c_{0,n_q}\phi_0(u)|n_q\rangle. \tag{43}$$

Figure 2 shows typical occupation probabilities of the basis states obtained by diagonalization of H_c for the $\omega_0 \approx 0$ case. If ω and λ' are about the same then the diagonal of the (n_u, n_q) matrix dominates [Fig. 2(a)]. The checkerboard pattern is due to the odd-even coupling between the u and q coordinates in Eq. (40). If $\lambda' \ll \omega$ then the q coordinate dominates and the larger n_q values are coupled with the lower n_u values [Fig. 2(b)]. On the other hand, for $\omega \ll \lambda'$ the u coordinate dominates and the n_u couples with the lower n_u-values [Fig. 2(c)]. This agrees with the results of the previous section.

IV. SOLUTION OF THE RELATIVE MOTION PART

We will use the SVM and the DFT approaches to calculate the wave function of the relative motion. These approaches are briefly described in the following.

A. SVM approach

In this approach the spatial part of the wave function is expanded into explicitly correlated Gaussians

$$\Phi_k(\mathbf{x}) = \mathcal{A}\left\{ e^{-\frac{1}{2}\sum_{i<j}^{N}\alpha_{ij}^k(\mathbf{x}_i-\mathbf{x}_j)^2-\frac{1}{2}\sum_{i=1}^{N}\beta_i^k(\mathbf{x}_i-\mathbf{s}_i^k)^2}\chi_S\right\}, \tag{44}$$

where $\mathcal{A}$ is an antisymmetrizer, χ_S is the N electron spin function (coupling the spin to S), and α_{ij}^k, β_i^k and $\mathbf{s}_i^k$ are nonlinear parameters.

The necessary matrix elements can be analytically calculated [67,74]. The basis functions are optimized by selecting the best spatial basis parameters using the SVM. In the SVM, the basis functions are optimized by randomly generating a large number of candidates and selecting the ones that give the lowest energy [67,74]. The size of the basis can be increased by adding the best states one by one. Once a basis is generated it can be refined by replacing states with randomly selected better basis functions. This approach is very efficient in finding suitable basis functions.

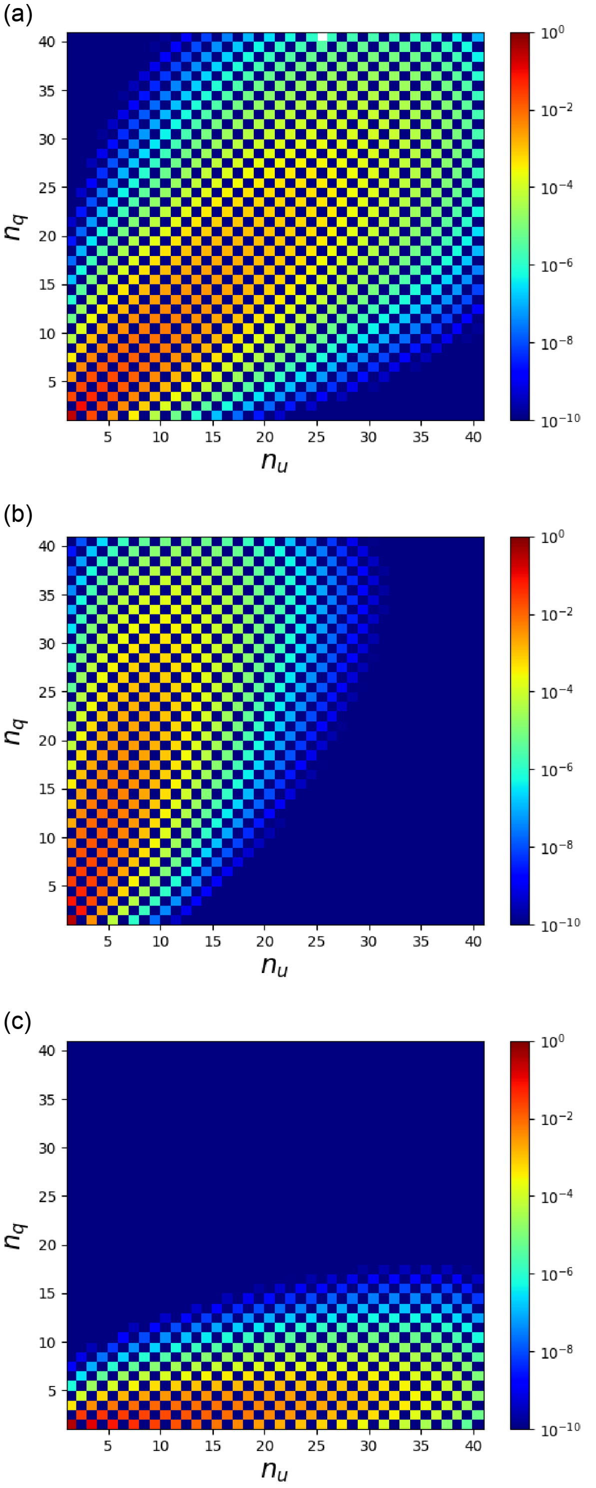

FIG. 2. Occupation probabilities for different parameters for the $\omega_0 \approx 0$ case. (a) $N = 50$, $\lambda = 0.1$ and $\omega = 1$, (b) $N = 50$, $\lambda = 0.1$, and $\omega = 10$. (c) $N = 500$, $\lambda = 0.1$ and $\omega = 1$.

B. DFT calculation

The DFT Hamiltonian is defined as

$$H_{\mathrm{x}}^{\mathrm{DFT}} = -\tfrac{1}{2}\nabla_{\mathbf{r}}^2 + V_H[\rho(\mathbf{r})] + V_{EX}[\rho_\uparrow(\mathbf{r}), \rho_\downarrow(\mathbf{r})] + V_c(\mathbf{r}), \tag{45}$$

TABLE I. Comparison of the energy of the relative motion calculated by SVM and DFT for different confinement strengths. S is the spin and N is the number of particles.

N	S	ω_0	DFT	SVM
2	0	0.5	1.743	1.659
		1.0	3.232	3.000
		1.5	4.626	4.268
2	1	0.5	1.980	1.913
		1.0	3.837	3.596
		1.5	5.627	5.236
3	0.5	0.5	3.703	3.583
		1.0	6.727	6.369
		1.5	9.544	8.982
3	1.5	0.5	3.840	3.714
		1.0	7.173	6.760
		1.5	10.34	9.681
4	0	0.5	6.074	6.071
		1.0	10.83	10.62
		1.5	15.23	14.57
4	1	0.5	6.049	5.964
		1.0	10.79	10.34
		1.5	15.18	14.48
4	2	0.5	6.493	6.349
		1.0	11.94	11.63
		1.5	17.10	16.27
5	0.5	0.5	8.905	8.880
		1.0	15.64	15.27
		1.5	21.81	21.39
5	1.5	0.5	9.092	9.074
		1.0	16.15	15.78
		1.5	22.67	22.04
5	2.5	0.5	9.476	9.287
		1.0	17.19	16.57
		1.5	24.45	23.50

where V_H is the Hartree, V_{EX} is the exchange correlation, V_c is the confining potential, and $\mathbf{r}$ is the single-particle coordinate of the electron. The local density approximation (LDA) is used for the exchange-correlation part and the system is spin polarized, $\rho = \rho_\uparrow + \rho_\downarrow$ with

$$\rho_\uparrow(\mathbf{r}) = \sum_i \phi_{\uparrow,i}(\mathbf{r})^2 \quad \rho_\downarrow(\mathbf{r}) = \sum_i \phi_{\downarrow,i}(\mathbf{r})^2, \tag{46}$$

where $\phi_\uparrow$ and $\phi_\downarrow$ are the Kohn-Sham orbitals of the spin-up and spin-down electrons, respectively. The DFT equations are solved on a numerical grid with finite difference representation of the kinetic energy operator and using a grid spacing of 0.2 a.u.

C. Numerical results

In this section we present numerical examples for the calculation of the energies and wave functions of the relative motion in two dimensions. The extension to three spatial dimension is straightforward. The energies calculated by SVM and DFT show similar trends as a function of the number of particles and spin symmetry (Table I). The SVM energies are accurate upper bounds of the exact energy and are always found to be smaller than the DFT ones. The DFT and SVM electron densities (see Fig. 3) are similar. The SVM and DFT figures are rotated with respect to each other because the ground state is rotationally invariant [due to the choice of $\boldsymbol{\lambda} = \lambda(1, 1, 0)$] and there is no preferred direction. The SVM and the DFT finds different, but equivalent rotated states.

The SVM energies are accurate and converged up to the digits shown. A more sophisticated exchange-correlation potential would perhaps improve the agreement between the SVM and DFT energies. The energy of the relative motion only adds a constant shift to the total energy for a given electron number, N, independently from λ and ω, and therefore its accurate value is somewhat less important. The SVM and DFT numbers follow the same trend as a function of spin and electron numbers and the energy differences by adding or removing an electron between appropriate spin states are very similar.

Figure 4 shows the DFT energy as a function of the number of electrons. The figure shows the energy for a spin 0 cases and one can see a smooth increase of energy with the increase of the number of electrons.

V. SUMMARY

We have shown that by decoupling the relative and the center-of-mass motion the energy and wave function of a confined N-electron system in an optical cavity can be straightforwardly calculated. The relative Hamiltonian has to be solved with a numerical approach, the light coupled CM motion can be solved analytically or by exact diagonalization. The advantage of the former is that the energy is analytical and simple, but the eigenfunctions are shifted Fock states depending on both the spatial and photon coordinates. The advantage of the latter is that the eigenfunctions are defined as products of spatial and photon basis states, which gives a more explicit physical picture of the spatial and photon space probability amplitudes in the wave function.

The relative wave function is completely decoupled from the light and can be solved with suitable approximations or numerical methods. In this work, we have used the SVM and the DFT approaches. The SVM is limited to few-electron systems because it explicitly antisymmetrizes the trial functions and the $N!$ scaling becomes prohibitively expensive for larger N. For few electrons, however, the SVM is very accurate, providing benchmark results for DFT and other approaches. The DFT can be easily used for larger systems, even for hundreds of electrons. In the present work, we have considered systems up to 100 electrons. The comparison of the energies and densities of the DFT and SVM calculations shows that the DFT predicts reasonable energies on the spin-polarized LDA level. The energy of the relative Hamiltonian only shifts the energy of the system, and it is independent of λ and ω.

The effective coupling strength depends on the number of particles and that offers an interesting possibility of tuning the transition energies and resonance parameters by changing the number of particles. The electron number also changes the relative importance of ω and λ, and one can selectively excite

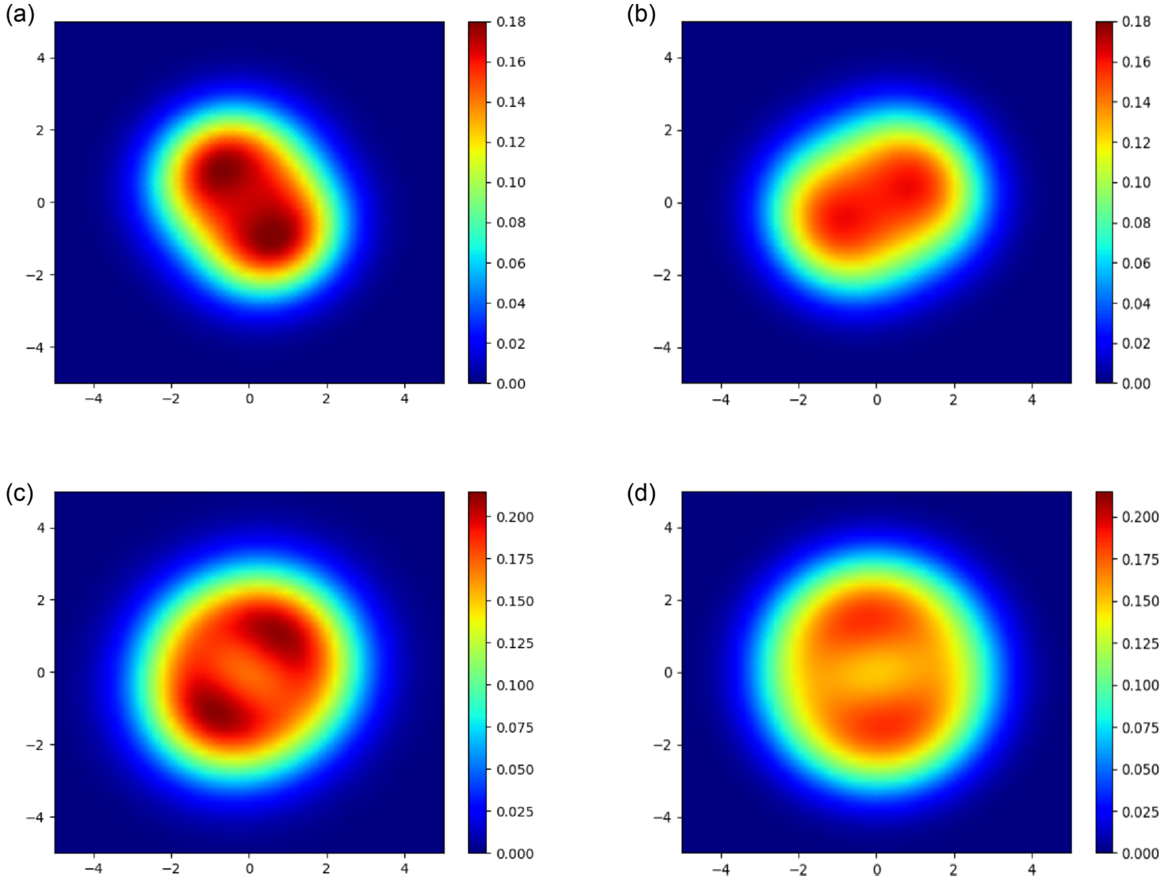

FIG. 3. Electron density for three electrons (a) SVM, (b) DFT and five electrons (c) SVM, (d) DFT for $\omega_0 = 0.5$.

spatial or photonic components by changing the number of electrons in the system.

The present approach can also be extended to a time-dependent Hamiltonian to work out an analytical solution for real-time dynamics as a possible benchmark for QED time-dependent DFT calculations. We plan to work on that problem in the future.

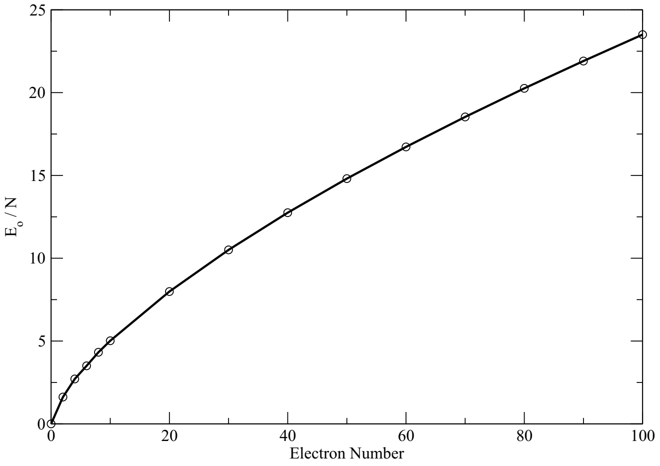

FIG. 4. Energy per electron in harmonically confined N-electron system calculated by DFT.

ACKNOWLEDGMENT

This work has been supported by the National Science Foundation (NSF) under Grant No. IRES 1826917.

Y.A. and J.M. equally contributed to this work.

APPENDIX: DECOUPLING THE PHOTONS IN THE MULTIPHOTON MODES CASE

$$H_c = -\frac{1}{2}\frac{\partial}{\partial u^2} + \frac{1}{2}\omega_u^2 u^2 + \sum_{i=1}^{Np}\bigg(-\frac{1}{2}\frac{\partial}{\partial q_i^2} + \frac{1}{2}\omega_i^2 q_i^2 - \sqrt{2N}\omega_i\lambda_i u q_i\bigg). \tag{A1}$$

We can introduce the substitutions, $u = \frac{u_i}{\sqrt{Np}}$, $\omega_{u_i} = \frac{\omega_u}{Np}$ This simplifies our Hamiltonian into the following,

$$H_c = \sum_{i=1}^{Np}\bigg(-\frac{1}{2}\frac{\partial}{\partial u_i{}^2} + \frac{1}{2}\omega_{u_i}^2 u_i{}^2 - \frac{1}{2}\frac{\partial}{\partial q_i^2} + \frac{1}{2}\omega_i^2 q_i^2 - \sqrt{2N}\omega_i\lambda_i u_i q_i\bigg), \tag{A2}$$

which can be written in the form,

$$H_c = \sum_{i=1}^{Np} H_{c_i}, \tag{A3}$$

where

$$H_{c_i} = -\frac{1}{2}\frac{\partial}{\partial {u_i}^2} + \frac{1}{2}\omega_{u_i}^2 {u_i}^2 - \frac{1}{2}\frac{\partial}{\partial q_i^2} + \frac{1}{2}\omega_i^2 q_i^2 - \sqrt{2N}\omega_i\lambda_i u_i q_i. \tag{A4}$$

We can then separate out each of the H_{c_i} and solve them individually. We once again use the following shifted Fock states,

$$s_i = u_i sin(\alpha_i) + q_i \cos(\alpha_i) \tag{A5}$$

$$t_i = -u_i \cos(\alpha_i) + q_i \sin(\alpha_i). \tag{A6}$$

Setting

$$\tan(2\alpha_i) = \frac{2\sqrt{2N}\omega_i\lambda_i}{\chi_i}, \quad \chi_i = \omega_{u_i}^2 - \omega_i^2 \tag{A7}$$

we can ensure the coupling term of the Hamiltonian is eliminated. As a result, the Hamiltonian simplifies to,

$$H_{c_i} = -\frac{1}{2}\frac{\partial}{\partial {s_i}^2} + \frac{1}{2}\omega_{s_i}^2 {s_i}^2 - \frac{1}{2}\frac{\partial}{\partial {t_i}^2} + \frac{1}{2}\omega_{t_i}^2 {t_i}^2, \tag{A8}$$

where

$$\omega_{s_i} = |\sin(\alpha_i)|\sqrt{\omega_{u_i}^2 + \frac{\omega_i^2}{\tan^2(\alpha_i)} - \frac{2\sqrt{2N}\omega_i\lambda_i}{\tan(\alpha_i)}} \tag{A9}$$

$$\omega_{t_i} = |\cos(\alpha_i)|\sqrt{\omega_{u_i}^2 + \omega_i^2\tan^2(\alpha_i) + 2\sqrt{2N}\omega_i\lambda_i\tan(\alpha_i)}, \tag{A10}$$

where $\omega_{u_i}^2 = \frac{\omega_0^2 + 2N\lambda^2}{N_p^2}$.

[1] J. Feist and F. J. Garcia-Vidal, Extraordinary Exciton Conductance Induced by Strong Coupling, Phys. Rev. Lett. **114**, 196402 (2015).

[2] R. Balili, V. Hartwell, D. Snoke, L. Pfeiffer, and K. West, Bose-einstein condensation of microcavity polaritons in a trap, Science **316**, 1007 (2007).

[3] J. Schachenmayer, C. Genes, E. Tignone, and G. Pupillo, Cavity-Enhanced Transport of Excitons, Phys. Rev. Lett. **114**, 196403 (2015).

[4] B. Xiang, R. F. Ribeiro, M. Du, L. Chen, Z. Yang, J. Wang, J. Yuen-Zhou, and W. Xiong, Intermolecular vibrational energy transfer enabled by microcavity strong light–matter coupling, Science **368**, 665 (2020).

[5] A. Reserbat-Plantey, I. Epstein, I. Torre, A. T. Costa, P. A. D. Gonalves, N. A. Mortensen, M. Polini, J. C. W. Song, N. M. R. Peres, and F. H. L. Koppens, Quantum nanophotonics in two-dimensional materials, ACS Photon. **8**, 85 (2021).

[6] D. M. Coles, N. Somaschi, P. Michetti, C. Clark, P. G. Lagoudakis, P. G. Savvidis, and D. G. Lidzey, Polariton-mediated energy transfer between organic dyes in a strongly coupled optical microcavity, Nat. Mater. **13**, 712 (2014).

[7] J. Kasprzak, M. Richard, S. Kundermann, A. Baas, P. Jeambrun, J. M. J. Keeling, F. M. Marchetti, M. H. Szymańska, R. André, J. L. Staehli, V. Savona, P. B. Littlewood, B. Deveaud, and L. S. Dang, Bose–einstein condensation of exciton polaritons, Nature (London) **443**, 409 (2006).

[8] T. Schwartz, J. A. Hutchison, C. Genet, and T. W. Ebbesen, Reversible Switching of Ultrastrong Light-Molecule Coupling, Phys. Rev. Lett. **106**, 196405 (2011).

[9] J. D. Plumhof, T. Stöferle, L. Mai, U. Scherf, and R. F. Mahrt, Room-temperature bose–einstein condensation of cavity exciton–polaritons in a polymer, Nat. Mater. **13**, 247 (2014).

[10] J. A. Hutchison, A. Liscio, T. Schwartz, A. Canaguier-Durand, C. Genet, V. Palermo, P. Samorì, and T. W. Ebbesen, Tuning the work-function via strong coupling, Adv. Mater. **25**, 2481 (2013).

[11] K. Wang, M. Seidel, K. Nagarajan, T. Chervy, C. Genet, and T. Ebbesen, Large optical nonlinearity enhancement under electronic strong coupling, Nat. Commun. **12**, 1486 (2021).

[12] D. N. Basov, A. Asenjo-Garcia, P. J. Schuck, X. Zhu, and A. Rubio, Polariton panorama, Nanophotonics **10**, 549 (2021).

[13] G. Mazza and A. Georges, Superradiant Quantum Materials, Phys. Rev. Lett. **122**, 017401 (2019).

[14] O. Di Stefano, A. Settineri, V. Macrì, L. Garziano, R. Stassi, S. Savasta, and F. Nori, Resolution of gauge ambiguities in ultrastrong-coupling cavity quantum electrodynamics, Nat. Phys. **15**, 803 (2019).

[15] J. Galego, F. J. Garcia-Vidal, and J. Feist, Cavity-Induced Modifications of Molecular Structure in the Strong-Coupling Regime, Phys. Rev. X **5**, 041022 (2015).

[16] F. Herrera and F. C. Spano, Cavity-Controlled Chemistry in Molecular Ensembles, Phys. Rev. Lett. **116**, 238301 (2016).

[17] J. Galego, F. J. Garcia-Vidal, and J. Feist, Suppressing photochemical reactions with quantized light fields, Nat. Commun. **7**, 13841 (2016).

[18] A. Shalabney, J. George, J. Hutchison, G. Pupillo, C. Genet, and T. W. Ebbesen, Coherent coupling of molecular resonators with a microcavity mode, Nature Commun. **6**, 5981 (2015).

[19] F. Buchholz, I. Theophilou, S. E. B. Nielsen, M. Ruggenthaler, and A. Rubio, Reduced density-matrix approach to strong matter-photon interaction, ACS Photon. **6**, 2694 (2019).

[20] C. Schäfer, M. Ruggenthaler, H. Appel, and A. Rubio, Modification of excitation and charge transfer in cavity quantum-electrodynamical chemistry, Proc. Natl. Acad. Sci. USA **116**, 4883 (2019).

[21] M. Ruggenthaler, N. Tancogne-Dejean, J. Flick, H. Appel, and A. Rubio, From a quantum-electrodynamical light–matter description to novel spectroscopies, Nature Rev. Chem. **2**, 0118 (2018).

[22] J. Flick, M. Ruggenthaler, H. Appel, and A. Rubio, Kohn–sham approach to quantum electrodynamical density-functional theory: Exact time-dependent effective potentials in real space, Proc. Natl. Acad. Sci. USA **112**, 15285 (2015).

[23] J. Flick, M. Ruggenthaler, H. Appel, and A. Rubio, Atoms and molecules in cavities, from weak to strong coupling in quantum-electrodynamics (qed) chemistry, Proc. Natl. Acad. Sci. USA **114**, 3026 (2017).

[24] L. Lacombe, N. M. Hoffmann, and N. T. Maitra, Exact Potential Energy Surface for Molecules in Cavities, Phys. Rev. Lett. **123**, 083201 (2019).

[25] A. Mandal, S. Montillo Vega, and P. Huo, Polarized fock states and the dynamical casimir effect in molecular cavity quantum electrodynamics, J. Phys. Chem. Lett. **11**, 9215 (2020).

[26] J. Flick, D. M. Welakuh, M. Ruggenthaler, H. Appel, and A. Rubio, Lightmatter response in nonrelativistic quantum electrodynamics, ACS Photon. **6**, 2757 (2019).

[27] S. Latini, E. Ronca, U. De Giovannini, H. Hübener, and A. Rubio, Cavity control of excitons in two-dimensional materials, Nano Lett. **19**, 3473 (2019).

[28] J. Flick, N. Rivera, and P. Narang, Strong light-matter coupling in quantum chemistry and quantum photonics, Nanophotonics **7**, 1479 (2018).

[29] J. Flick and P. Narang, Cavity-Correlated Electron-Nuclear Dynamics from First Principles, Phys. Rev. Lett. **121**, 113002 (2018).

[30] F. J. Garcia-Vidal, C. Ciuti, and T. W. Ebbesen, Manipulating matter by strong coupling to vacuum fields, Science **373**, 1126 (2021).

[31] A. Thomas, L. Lethuillier-Karl, K. Nagarajan, R. M. A. Vergauwe, J. George, T. Chervy, A. Shalabney, E. Devaux, C. Genet, J. Moran, and T. W. Ebbesen, Tilting a ground-state reactivity landscape by vibrational strong coupling, Science **363**, 615 (2019).

[32] U. Mordovina, C. Bungey, H. Appel, P. J. Knowles, A. Rubio, and F. R. Manby, Polaritonic coupled-cluster theory, Phys. Rev. Res. **2**, 023262 (2020).

[33] D. S. Wang, T. Neuman, J. Flick, and P. Narang, Lightmatter interaction of a molecule in a dissipative cavity from first principles, J. Chem. Phys. **154**, 104109 (2021).

[34] A. E. DePrince, Cavity-modulated ionization potentials and electron affinities from quantum electrodynamics coupled-cluster theory, J. Chem. Phys. **154**, 094112 (2021).

[35] T. S. Haugland, C. Schäfer, E. Ronca, A. Rubio, and H. Koch, Intermolecular interactions in optical cavities: An ab initio qed study, J. Chem. Phys. **154**, 094113 (2021).

[36] N. M. Hoffmann, L. Lacombe, A. Rubio, and N. T. Maitra, Effect of many modes on self-polarization and photochemical suppression in cavities, J. Chem. Phys. **153**, 104103 (2020).

[37] J. Flick and P. Narang, Ab initio polaritonic potential-energy surfaces for excited-state nanophotonics and polaritonic chemistry, J. Chem. Phys. **153**, 094116 (2020).

[38] A. Mandal, T. D. Krauss, and P. Huo, Polariton-mediated electron transfer via cavity quantum electrodynamics, J. Phys. Chem. B **124**, 6321 (2020).

[39] J. Galego, F. J. Garcia-Vidal, and J. Feist, Many-Molecule Reaction Triggered by a Single Photon in Polaritonic Chemistry, Phys. Rev. Lett. **119**, 136001 (2017).

[40] J. Flick, C. Schäfer, M. Ruggenthaler, H. Appel, and A. Rubio, Ab initio optimized effective potentials for real molecules in optical cavities: Photon contributions to the molecular ground state, ACS Photon. **5**, 992 (2018).

[41] C. Schäfer, M. Ruggenthaler, and A. Rubio, Ab initio nonrelativistic quantum electrodynamics: Bridging quantum chemistry and quantum optics from weak to strong coupling, Phys. Rev. A **98**, 043801 (2018).

[42] D. Sidler, M. Ruggenthaler, H. Appel, and A. Rubio, Chemistry in quantum cavities: Exact results, the impact of thermal velocities, and modified dissociation, J. Phys. Chem. Lett. **11**, 7525 (2020).

[43] I. Theophilou, M. Penz, M. Ruggenthaler, and A. Rubio, Virial relations for electrons coupled to quantum field modes, J. Chem. Theory Comput. **16**, 6236 (2020).

[44] D. Sidler, C. Schäfer, M. Ruggenthaler, and A. Rubio, Polaritonic chemistry: Collective strong coupling implies strong local modification of chemical properties, J. Phys. Chem. Lett. **12**, 508 (2021).

[45] F. Buchholz, I. Theophilou, K. J. H. Giesbertz, M. Ruggenthaler, and A. Rubio, Lightmatter hybrid-orbital-based first-principles methods: The influence of polariton statistics, J. Chem. Theory Comput. **16**, 5601 (2020).

[46] I. V. Tokatly, Conserving approximations in cavity quantum electrodynamics: Implications for density functional theory of electron-photon systems, Phys. Rev. B **98**, 235123 (2018).

[47] N. Rivera, J. Flick, and P. Narang, Variational Theory of Nonrelativistic Quantum Electrodynamics, Phys. Rev. Lett. **122**, 193603 (2019).

[48] T. Szidarovszky, G. J. Halász, and Á. Vibók, Three-player polaritons: nonadiabatic fingerprints in an entangled atom–molecule–photon system, New J. Phys. **22**, 053001 (2020).

[49] L. S. Cederbaum, Polaritonic states of matter in a rotating cavity, J. Phys. Chem. Lett. **12**, 6056 (2021).

[50] E. T. Jaynes and F. W. Cummings, Comparison of quantum and semiclassical radiation theories with application to the beam maser, Proc. IEEE **51**, 89 (1963).

[51] V. Rokaj, D. M. Welakuh, M. Ruggenthaler, and A. Rubio, Light–matter interaction in the long-wavelength limit: No ground-state without dipole self-energy, J. Phys. B: At. Mol. Opt. Phys. **51**, 034005 (2018).

[52] L. S. Cederbaum and A. I. Kuleff, Impact of cavity on interatomic coulombic decay, Nat. Commun. **12**, 4083 (2021).

[53] T. Szidarovszky, G. J. Halász, A. G. Császár, L. S. Cederbaum, and A. Vibók, Conical intersections induced by quantum light: Field-dressed spectra from the weak to the ultrastrong coupling regimes, J. Phys. Chem. Lett. **9**, 6215 (2018).

[54] Y. Ashida, A. İmamoğlu, and E. Demler, Cavity Quantum Electrodynamics at Arbitrary Light-Matter Coupling Strengths, Phys. Rev. Lett. **126**, 153603 (2021).

[55] P. A. Maksym and T. Chakraborty, Quantum Dots in a Magnetic Field: Role of Electron-Electron Interactions, Phys. Rev. Lett. **65**, 108 (1990).

[56] T.-L. Ho and Q. Zhou, Obtaining the phase diagram and thermodynamic quantities of bulk systems from the densities of trapped gases, Nat. Phys. **6**, 131 (2010).

[57] A. L. Gaunt, T. F. Schmidutz, I. Gotlibovych, R. P. Smith, and Z. Hadzibabic, Bose-Einstein Condensation of Atoms in a Uniform Potential, Phys. Rev. Lett. **110**, 200406 (2013).

[58] T. Yefsah, R. Desbuquois, L. Chomaz, K. J. Günter, and J. Dalibard, Exploring the Thermodynamics of a Two-Dimensional Bose Gas, Phys. Rev. Lett. **107**, 130401 (2011).

[59] W. Kohn, Cyclotron resonance and de haas-van alphen oscillations of an interacting electron gas, Phys. Rev. **123**, 1242 (1961).

[60] S. K. Yip, Magneto-optical absorption by electrons in the presence of parabolic confinement potentials, Phys. Rev. B **43**, 1707 (1991).

[61] I. V. Tokatly, Time-Dependent Density Functional Theory for Many-Electron Systems Interacting with Cavity Photons, Phys. Rev. Lett. **110**, 233001 (2013).

[62] G. Vignale, Center of Mass and Relative Motion in Time Dependent Density Functional Theory, Phys. Rev. Lett. **74**, 3233 (1995).

[63] L. Brey, N. F. Johnson, and B. I. Halperin, Optical and magneto-optical absorption in parabolic quantum wells, Phys. Rev. B **40**, 10647 (1989).

[64] J. F. Dobson, Harmonic-Potential Theorem: Implications for Approximate Many-Body Theories, Phys. Rev. Lett. **73**, 2244 (1994).

[65] C. Huang, A. Ahrens, M. Beutel, and K. Varga, Two electrons in harmonic confinement coupled to light in a cavity, Phys. Rev. B **104**, 165147 (2021).

[66] M. Taut, Two electrons in an external oscillator potential: Particular analytic solutions of a coulomb correlation problem, Phys. Rev. A **48**, 3561 (1993).

[67] Y. Suzuki, M. Suzuki, and K. Varga, *Stochastic Variational Approach to Quantum-Mechanical Few-Body Problems*, Vol. 54 (Springer Science & Business Media, Berlin, 1998).

[68] K. Varga, P. Navratil, J. Usukura, and Y. Suzuki, Stochastic variational approach to few-electron artificial atoms, Phys. Rev. B **63**, 205308 (2001).

[69] J. Usukura, Y. Suzuki, and K. Varga, Stability of two- and three-dimensional excitonic complexes, Phys. Rev. B **59**, 5652 (1999).

[70] C. Riva, F. M. Peeters, and K. Varga, Excitons and charged excitons in semiconductor quantum wells, Phys. Rev. B **61**, 13873 (2000).

[71] D. K. Zhang, D. W. Kidd, and K. Varga, Excited biexcitons in transition metal dichalcogenides, Nano Lett. **15**, 7002 (2015).

[72] D. W. Kidd, D. K. Zhang, and K. Varga, Binding energies and structures of two-dimensional excitonic complexes in transition metal dichalcogenides, Phys. Rev. B **93**, 125423 (2016).

[73] A. Ahrens, C. Huang, M. Beutel, C. Covington, and K. Varga, Stochastic Variational Approach to Small Atoms and Molecules Coupled to Quantum Field Modes in Cavity QED, Phys. Rev. Lett. **127**, 273601 (2021).

[74] J. Mitroy, S. Bubin, W. Horiuchi, Y. Suzuki, L. Adamowicz, W. Cencek, K. Szalewicz, J. Komasa, D. Blume, and K. Varga, Theory and application of explicitly correlated gaussians, Rev. Mod. Phys. **85**, 693 (2013).

[75] T. Zaklama, D. Zhang, K. Rowan, L. Schatzki, Y. Suzuki, and K. Varga, Matrix elements of one dimensional explicitly correlated gaussian basis functions, Few-Body Syst. **61**, 6 (2020).

[76] T. Joyce and K. Varga, Matrix elements of explicitly correlated gaussian basis functions with arbitrary angular momentum, J. Chem. Phys. **144**, 184106 (2016).

[77] M. Beutel, A. Ahrens, C. Huang, Y. Suzuki, and K. Varga, Deformed explicitly correlated gaussians, J. Chem. Phys. **155**, 214103 (2021).

[78] J.-Y. Zhang, J. Mitroy, and K. Varga, Positron Scattering and Annihilation from the Hydrogen Molecule at Zero Energy, Phys. Rev. Lett. **103**, 223202 (2009).

[79] J.-Y. Zhang, M.-S. Wu, Y. Qian, X. Gao, Y.-J. Yang, K. Varga, Z.-C. Yan, and U. Schwingenschlogl, *s*-wave elastic scattering of *o*-ps from H_2 at low energy, Phys. Rev. A **100**, 032701 (2019).

[80] K. Varga, Multipositronic Systems, Phys. Rev. Lett. **83**, 5471 (1999).

[81] P. Hohenberg and W. Kohn, Inhomogeneous electron gas, Phys. Rev. **136**, B864 (1964).

[82] W. Kohn and L. J. Sham, Self-consistent equations including exchange and correlation effects, Phys. Rev. **140**, A1133 (1965).

[83] E. Räsänen, H. Saarikoski, V. N. Stavrou, A. Harju, M. J. Puska, and R. M. Nieminen, Electronic structure of rectangular quantum dots, Phys. Rev. B **67**, 235307 (2003).

[84] H. Jiang, H. U. Baranger, and W. Yang, Density-functional theory simulation of large quantum dots, Phys. Rev. B **68**, 165337 (2003).

[85] K. Kärkkäinen, M. Koskinen, S. M. Reimann, and M. Manninen, Density-functional theory of multicomponent quantum dots, Phys. Rev. B **70**, 195310 (2004).

[86] L. K. Castelano, G.-Q. Hai, B. Partoens, and F. M. Peeters, Artificial molecular quantum rings: Spin density functional theory calculations, Phys. Rev. B **74**, 045313 (2006).

[87] M. Koskinen, M. Manninen, and S. M. Reimann, Hund's Rules and Spin Density Waves in Quantum Dots, Phys. Rev. Lett. **79**, 1389 (1997).

[88] S. Pittalis and E. Räsänen, Orbital-free energy functional for electrons in two dimensions, Phys. Rev. B **80**, 165112 (2009).

[89] C. Huang, D. Pitagora, T. Zaklama, and K. Varga, Energy spectrum and structure of confined one-dimensional few-electron systems with and without coupling to light in a cavity, Phys. Rev. A **104**, 043109 (2021).

[90] M. Ruggenthaler, J. Flick, C. Pellegrini, H. Appel, I. V. Tokatly, and A. Rubio, Quantum-electrodynamical density-functional theory: Bridging quantum optics and electronic-structure theory, Phys. Rev. A **90**, 012508 (2014).